Palaeogeography, Palaeoclimatology, Palaeoecology 373 (2013) 152–162

Contents lists available at SciVerse ScienceDirect

Palaeogeography, Palaeoclimatology, Palaeoecology

journal homepage: www.elsevier.com/locate/palaeo

Climate signatures on decadal to interdecadal time scales as obtained from mollusk shells (*Arctica islandica*) from Iceland

Gerrit Lohmann [a,*], Bernd R. Schöne [b]

[a] Alfred Wegener Institute for Polar and Marine Research, Bussestr. 24, 27570 Bremerhaven, Germany
[b] Institute of Geosciences, Earth System Science Research Center, University of Mainz, Johann-Joachim-Becher-Weg 21, 55128 Mainz, Germany

ARTICLE INFO

Article history:
Received 1 November 2011
Received in revised form 4 August 2012
Accepted 12 August 2012
Available online 13 September 2012

Keywords:
Climate proxy
North Atlantic climate variability
Teleconnections
Proxy data
Atmospheric circulation

ABSTRACT

Pronounced decadal climate oscillations are detected in a multi-centennial record based on shell growth rates of the marine bivalve mollusk, *Arctica islandica*, from Iceland. The corresponding analysis of patterns in sea level pressure and temperature exhibit large-scale teleconnections with North Atlantic climate quantities. We find that the record projects onto blocking situations in the northern North Atlantic. The associated circulation shows a low-pressure signature over Greenland and the Labrador Sea and a high-pressure system over Western Europe associated with northeasterly flow towards Iceland and weakening in the westerly zonal flow over Europe. It can be speculated that such circulation affects food availability controlling shell growth. On multidecadal time scales, the record shows a pronounced variability linked to North Atlantic temperature. In our record, we find enhanced variability of the shell growth rates on multidecadal time scales, and it appears that this oscillation has high amplitudes in the 16th to 18th century also consistent with marine alkenone data. It is conceivable that these climate oscillations, also linked to sea ice export and enhanced blocking, are a more pronounced feature during times when the climate was relatively cold.

1. Introduction

In order to attribute recent environmental changes to human influence knowledge of the background variability is required, particularly for the latest Holocene (Jansen et al., 2007). Instrumental and proxy data indicate that the climate over the North Atlantic sector varies largely on quasi-decadal to multi-decadal time scales (Deser and Blackmon, 1993; Hurrell, 1995; Enfield and Mayer, 1997; Sutton and Allen, 1997; Dima and Lohmann, 2007). Decadal variability in the North Atlantic is characterized by a tripole pattern in sea surface temperature (SST) anomalies and is linked to atmosphere–ocean interactions (Bjerknes, 1964; Deser and Blackmon, 1993; Kushnir, 1994; Dima and Lohmann, 2004). Part of its signature resembles the North Atlantic Oscillation (NAO) (Hurrell and van Loon, 1997) pattern. Teleconnection patterns are large-scale patterns associated to atmosphere–ocean dynamics (for a review: Barnston and Livezey, 1987). A primary objective of paleoclimate research is the reconstruction and characterization of natural climate variability. Based on the relationships between atmospheric teleconnection patterns and different proxy data during the observational period, valuable information related to the NAO and its associated climate anomalies during the pre-instrumental period has been obtained (e.g. Appenzeller et al., 1998; Trouet et al., 2009; Rimbu and Lohmann, 2011). Teleconnection patterns, in particular the NAO and other modes in the North Atlantic are related to the frequency, intensity and spatial distribution of synoptic scale atmospheric phenomena, including atmospheric blocking (e.g., Shabbar et al., 2001). Therefore, decadal variations of atmospheric teleconnection pattern indices give information about decadal variations in the properties of synoptic-scale phenomena.

There is evidence that the global climate system contains modes of climatic variability operating on multidecadal time scales involving temperature and circulation (Mann et al., 1995; Delworth and Mann, 2000). The signature of multidecadal variability has been detected in observed sea surface temperature (SST) data showing a monopolar SST signature in the North Atlantic (Deser and Blackmon, 1993; Kushnir, 1994). The Atlantic Multidecadal Oscillation (AMO) was firstly detected from the instrumental data (Schlesinger and Ramankutty, 1994) and later on demonstrated to exist in both proxies (Mann et al., 1995; Lohmann et al., 2004; Grosfeld et al., 2007; Hetzinger et al., 2008; Poore et al., 2009; Knudsen et al., 2011) and climate models (Timmermann et al., 1998; Delworth and Mann, 2000; Latif et al., 2004; Knight et al., 2005). In control experiments of long-term simulations, the AMO has been considered as an internal mode of variability linked to reorganizations of the ocean meridional overturning circulation (e.g. Delworth and Mann, 2000; Wei et al., 2012). However, the temperature in the North Atlantic is additionally affected by external forcing through greenhouse gases, solar irradiance and volcanoes. It is worth noting that AMO also affects structures like NAO and blocking (Eden and Jung, 2001; Grosfeld et al., 2007; Häkkinen et al., 2011).

* Corresponding author. Tel.: +49 471 4831 1758 1760; fax: +49 471 4831 1797.
E-mail address: Gerrit.Lohmann@awi.de (G. Lohmann).

0031-0182/$ – see front matter © 2012 Published by Elsevier B.V.
http://dx.doi.org/10.1016/j.palaeo.2012.08.006

Ocean-based reconstructions of climate variability can be vital in verifying, comparing and linking various climate proxies (e.g., Kim et al., 2004). In addition, marine records are less affected by very regional features and small-scale noise in the system. As compared to terrestrial archives, oceans provide a long-term memory of the climate system (Hasselmann, 1974; Frankignoul and Hasselmann, 1977) and can act as a natural filter to detect large-scale climate variability modes.

Here, we present a proxy record of decadal climate oscillations over the last five centuries based on shell growth rates of the marine bivalve mollusk, *Arctica islandica* from Iceland (Schöne et al., 2005a). *A. islandica* is an extremely long-lived species (225 to over 500 years: Ropes and Murawski, 1983; Schöne et al., 2005a; Wanamaker et al., 2008) and exhibits a broad biogeographic distribution in the northern North Atlantic (Nicol, 1951; Dahlgren et al., 2000). More than anything, what makes *Arctica* an ideal paleoclimate archive is the fact that specimens of the same population grow at similar rates. This means that (a) shell growth is responding to a common signal and (b) annual growth increment time-series of specimens with overlapping life-spans can be crossdated and combined to a longer composite (or master) chronology that covers numerous generations and many centuries. Distinct growth lines form during fall (e.g., Jones, 1980; Weidman et al., 1994; Schöne, 2008) and separate the growth pattern into time slices of equal duration, so-called growth increments. Growth increments and lines enable precise calendar dating. Variation in increment width reflects environmental change. Usually, higher food availability results in faster shell growth (Gunter, 1957; Witbaard et al., 1997). The development of *A. islandica* as a climate archive has been discussed extensively (e.g., Butler et al., 2010; Marchitto et al., 2000; Schöne et al., 2005b; Wanamaker et al., 2009, 2011, 2012; Weidman et al., 1994).

2. Data and methods

Eleven specimens of *A. islandica* were collected alive by dredging from ~30 m water depth around Iceland (Table 1). Specimen M071868-A3 was used in Schöne et al. (2005a). To analyze internal annual growth patterns, digital images were taken from the Mutvei-stained (Schöne et al., 2005c) cross-sections of the shells using a Canon EOS 600D camera attached to an Olympus SZX16 binocular microscope equipped with sectoral dark field illumination (Schott VisiLED MC 1000). Annual increment widths were measured in the outer shell layer of the ventral margin and – to double-check the results – in the cardinal tooth portion in the direction of growth to the nearest 2 μm using the image analysis software Panopea (©Peinl and Schöne).

Table 1
List of shell used in the present study. All specimens were collected alive.

Specimen ID	Date of collection	Sample locality
Möller-A1	26 Nov 2003	N66°16′, W014°55.20′;
Möller-A2		Eiðisvík in Bakkafjörður,
Möller-A3		NE coast of Iceland
Möller-A4		
Möller-A5		
Möller-A6		
Möller-A7		
Möller-A9		
HM-Fla86-A1	Summer 1986	Unspecified (museum collection), near Flatey, North Iceland
M071868-A3	July 1868	Unspecified (museum collection),
M071868-A4		East Iceland

2.1. Age-detrending, crossdating, isolation of climate signals, composite chronology

For crossdating purposes and in order to isolate common climate signals from annual increment time-series growth trends related to ontogenetic age must be removed. As the bivalve grows older, the rate of calcium carbonate production and the year-to-year variance of the annual increment widths decrease (e.g. Jones, 1980; Jones et al., 1989). Such age-related trends were removed from measured annual increment width chronologies with statistical methods developed by dendrochronologists (Cook and Kairiukstis, 1990; Fritts, 1976).

The precise temporal alignment of the time-series (crossdating) was assessed with the COFECHA (Grissino-Mayer, 2001). This software preserves the high frequency variability of each chronology by using flexible cubic spline functions for detrending that closely approximate the measured data (high-pass filtering).

To isolate the common signal in contemporaneous specimens, however, two different low-pass filtering techniques were applied to estimate age-related growth trends (predicted growth values): a deterministic technique (power function) and a more flexible technique (cubic splines). Negative exponential functions turned out to be less useful as they do not faithfully capture the age-related growth trends of *A. islandica* from the studied localities. Regional curve standardization (RCS) (e.g., Esper et al., 2003) was not applied because this would require a much larger number of series.

We computed growth indices (GI) by dividing measured by predicted growth values for each year. The GI data were then (mathematically) standardized by subtracting the mean and dividing by the standard deviation of the GI time-series. This removes the high correlation between the mean and the variance from the

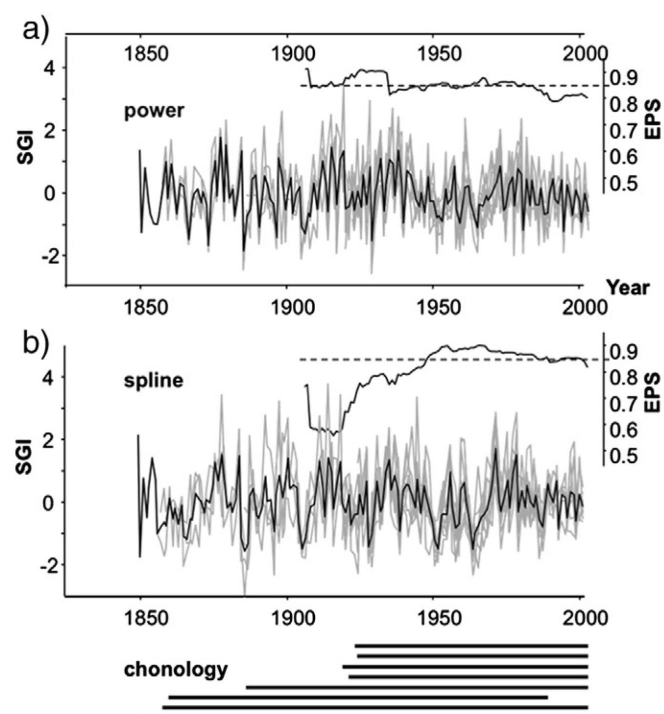

Fig. 1. Composite series of shell growth increments of the marine bivalve mollusk, *Arctica islandica* from northeast Iceland covering the last 150 years (based on Möller shells, NE Iceland, Table 1). A deterministic power function (a) and spline detrending (b) were applied as low-pass filtering techniques to estimate age-related growth trends. The composite chronologies are shown as the black line, the individual series in gray. EPS measures the appropriate inter-series correlation in running 50-year windows, i.e. the EPS value for 1950 is representative for 1900–1950. High EPS values indicate that the variance of a single SGI chronology sufficiently expresses the common variance of all SGI chronologies.

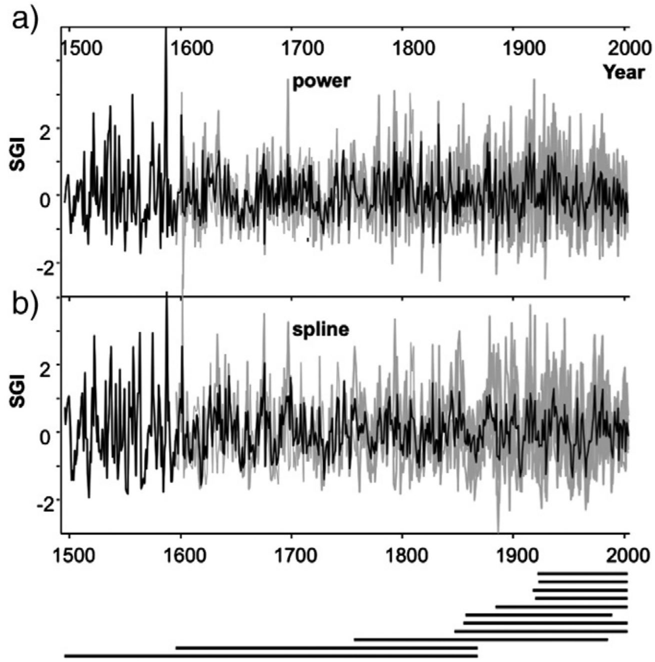

Fig. 2. As Fig. 1, but for 'All Iceland' covering the last 500 years (Table 1).

data (= heteroscedasticity). The standardized growth index (SGI) represents a dimensionless measure of how shell growth deviates from the estimated growth. Prior to further analyses, autocorrelation (lag-1) was removed from each of the SGI series (pre-whitening).

Finally, individual SGI series were combined in regional "composite" chronologies by calculating the arithmetic mean of the SGI values at each year. Fig. 1 shows "NE Iceland" based only on "Möller" shells (Table 1), Fig. 2 "All Iceland" are based on all specimens listed in Table 1. The strength of the composite chronology was assessed with the expressed population strength (EPS) value (Wigley et al., 1984):

$$EPS = n \cdot R_{bar} / (n \cdot R_{bar} + (1 - R_{bar})), \quad (1)$$

where R_{bar} is the average of all correlations between pairs of SGI time series and n is the number of specimens used to built the chronology. The EPS value quantifies the similarity between the averaged chronology and the theoretical 'infinitely replicated' chronology for the appropriate inter-series correlation (Briffa and Jones, 1990; Wigley et al., 1984). According to Wigley et al. (1984) EPS values greater than 0.85 indicate that the variance of a single SGI chronology sufficiently expresses the common variance of all SGI series. To demonstrate how the agreement between the SGI series changed through time, we computed EPS values in running 50-year windows (Fig. 1).

Possible climate impacts are investigated by analyzing the relation between SGI and gridded climate data sets. The spatial and temporal

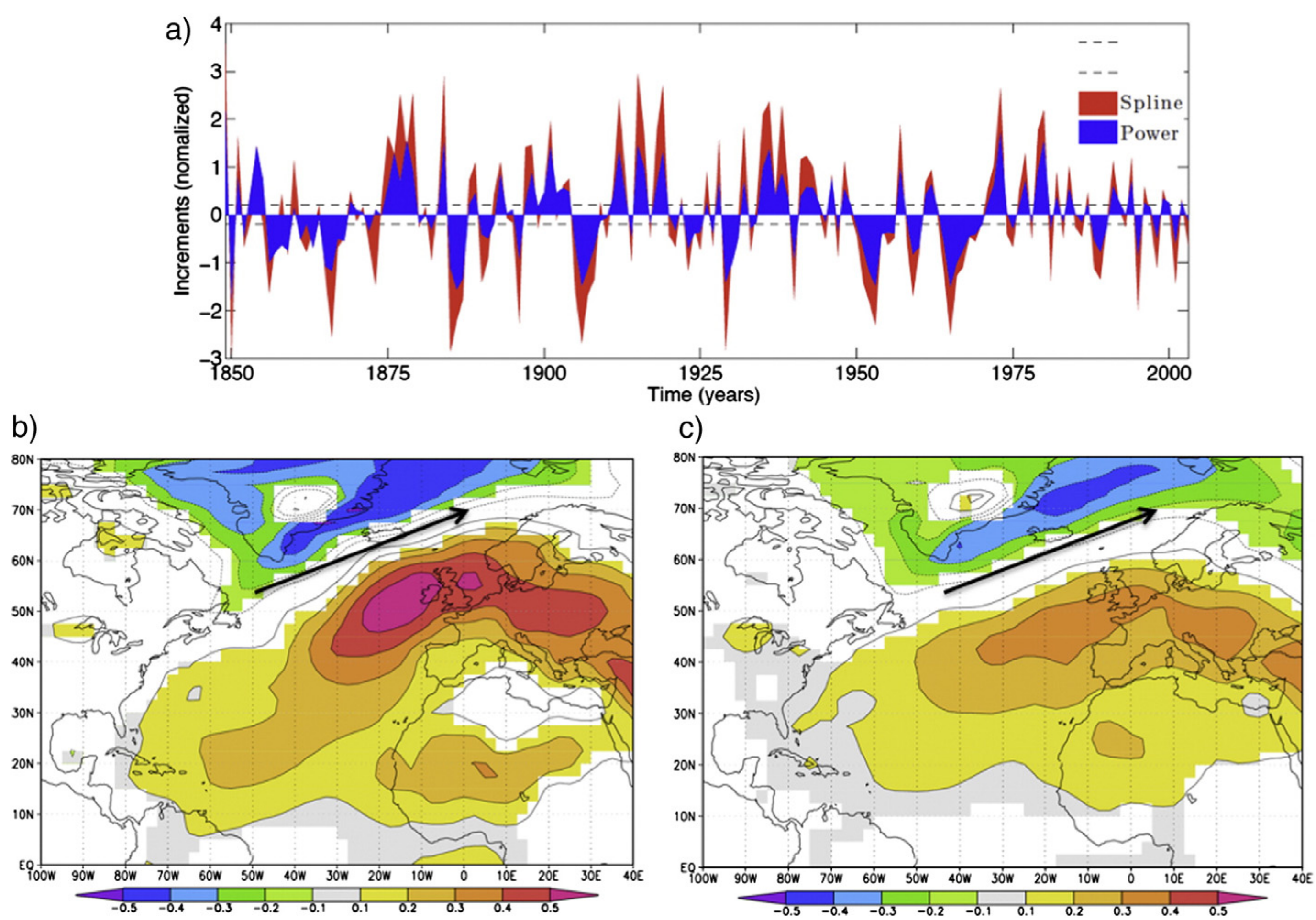

Fig. 3. a) Time series of master chronology shell growth increments of the marine bivalve mollusk, *Arctica islandica* from northeast Iceland covering the last 150 years (based on Möller shells, NE Iceland, Table 1). The dotted lines indicate the ±0.2 standard deviation which is used as threshold for our composite map analysis. Composite maps of SLP NCEP/NCAR with respect to SGI and threshold 0.2, i.e. all SLP maps are averaged when the SGI > 0.2 and are subtracted from the mean. b) Power, c) spline. Units are hPa. The flow goes from southeast to northeast of Iceland (arrows).

variability of the surface air temperature and sea level pressure (SLP) are represented by NCEP/NCAR reanalysis monthly mean data set, which uses a state-of-the-art analysis/forecast system to perform data assimilation using past data from 1948 to the present (Kalnay et al., 1996). The spatial resolution of the data set is 2.5°×2.5°. Furthermore, we make use of the updated SLP data set over the Northern Hemisphere for the period 1899–2003 (Trenberth and Paolino, 1980), as well as the Luterbacher et al. (2002) SLP fields over the eastern North Atlantic and Europe back to 1500. SLP is also taken from the 20th century reanalysis project (Compo et al., 2011) covering the period 1908–2008.

The Hadley Center Sea Ice and Sea Surface Temperature data set (HadISST2) (Rayner et al., 2006), taken from the Met Office Marine Data Bank (MDB), is analyzed to characterize the SST variability, and is a unique combination of monthly fields of SST and sea ice concentration on a 1°×1° latitude–longitude grid from 1870 to 2010.

Point correlation maps of the time series and climate fields are computed to investigate the spatial range of the relationships. To test the local significance of the correlations, we apply a double-sided significance test based on a t-distribution (von Storch and Zwiers, 1999) with $p = 0.05$. The significance of the correlation is established by using Monte Carlo experiments in which the same filter is applied to surrogate data ($N = 10{,}000$). In the correlation maps, areas of locally significant correlation are shaded.

To analyze relationships on multidecadal time scales, we apply a low-pass filter to the data prior to the correlation analyses. We use a finite response filter (cutoff frequency 1/30 years, length = 31 years; or 1/10 years, length = 11 years) with the boundary constraint of minimizing the first derivative (Mann, 2004). To assess the relationship between temperature, blocking and SGI, we calculate composite maps (von Storch and Zwiers, 1999). Here, all the composite maps are calculated by collecting the composite fields that are related to higher/lower SGI than a given threshold (±0.2) as indicated in Fig. 3a.

In the frequency domain, we apply a continuous wavelet analysis which intrinsically adjusts the time resolution to the analyzed scale (e.g., Torrence and Compo, 1998). Significance testing of wavelet spectra can be either through pointwise or areawise significance tests against reasonable background spectra (Maraun and Kurths, 2004; Torrence and Compo, 1998). The red noise background spectrum is calculated from an autoregressive process of first order autoregressive process AR(1) as null hypothesis (Hasselmann, 1976; von Storch and Zwiers, 1999).

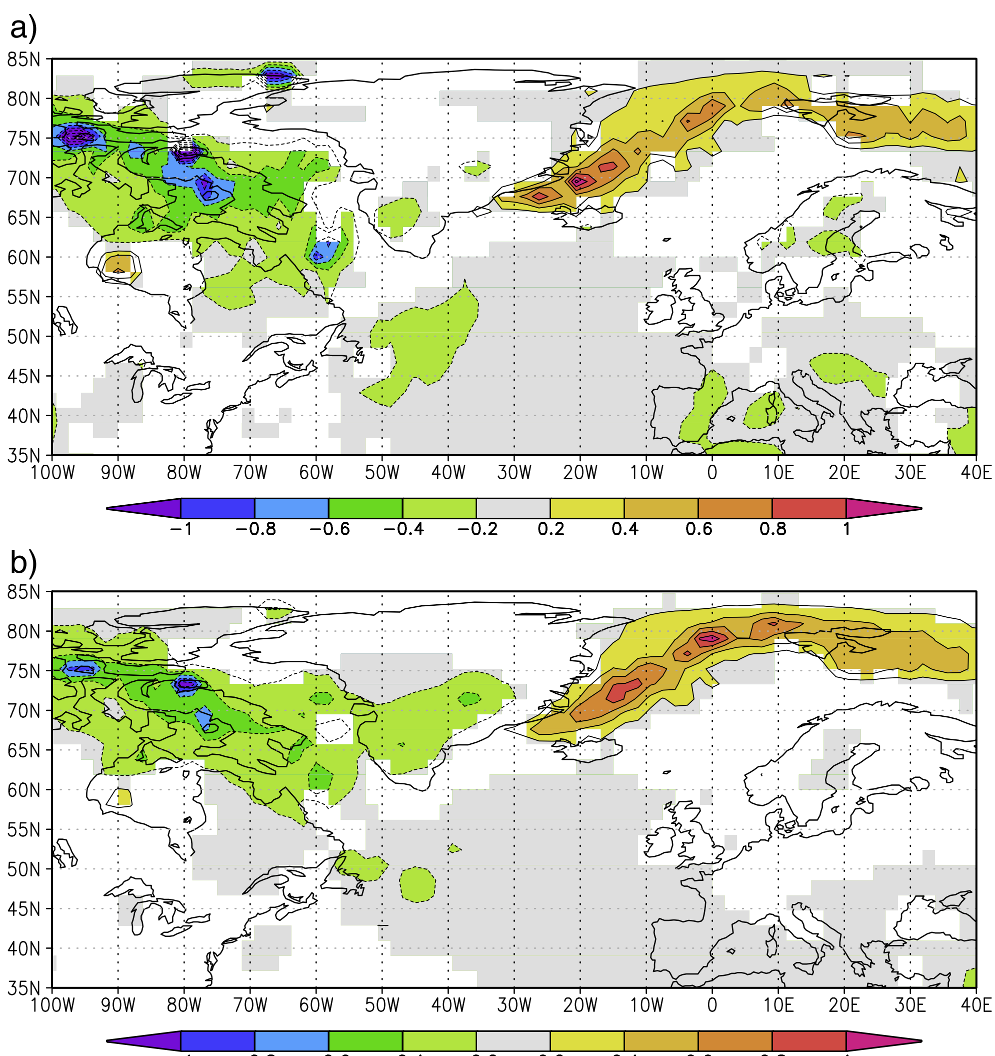

Fig. 4. Composite maps of surface temperature NCEP/NCAR with respect to SGI with threshold 0.2 in SGI, i.e. all SLP maps are averaged when the SGI > 0.2. a) Power, b) spline. Units are °C. High SGI is associated to anomalous warm temperatures north of Iceland and anomalous cold temperatures in the Baffin Bay and central Labrador Sea.

3. Results

The regional "NE Iceland" (Fig. 1) and multi-regional "All Iceland" (Fig. 2) composite chronologies cover the time intervals 1849 to 2003 AD and 1495 to 2003 AD, respectively. In case of the NE Iceland chronology, EPS values typically exceeded the threshold of 0.85 (or are close to 0.85) when at least three SGI series were available (Fig. 1). The EPS values are calculated for the period 1850 to 2003 AD, the value for 1950 is representative for the period 1900–1950. The two techniques (power and spline) provide similar results on decadal time scales (Fig. 1a, b). However, the EPS values are higher for the power than for the spline technique for the 50-year chunks prior to 1950. It will be seen later that the differences are of minor importance when analyzing the teleconnections. Fig. 2 shows the "All Iceland" chronology where both techniques retain most of the low frequency data (Figs. 2a, b). The concept of EPS values is not well suited before 1850 due to limited amount of data. Therefore, the SGI series shall be interpreted with caution as true master chronologies prior to 1850.

In order to understand the possible mechanisms behind the SGI record, we evaluate composite maps of SLP, SST, and sea ice fields. For the composite maps of SLP NCEP/NCAR with respect to SGI, we chose a threshold 0.2 (Fig. 3a), i.e. all SLP maps are averaged when the SGI > 0.2. Fig. 3b is related to the power, Fig. 3c to the spline construction of the index. This pattern is furthermore robust when changing the threshold. The flow pattern shows a typical blocking situation with a low pressure above eastern Greenland and a high-pressure center over Europe. Notice that the flow is along the pressure isobars: clockwise around a high, anti-clockwise around a low-pressure system. Regionally, the atmospheric circulation goes from southeast to northeast of Iceland (black arrows). A reverse pattern occurs during years with low increments in the shell, with the negative center displaced eastward (not shown). The results are also robust when taking other SLP data sets (Luterbacher et al., 2002; Trenberth and Paolino, 1980).

The associated wind field has a strong projection onto the Greenland Sea affecting temperature and other climate variables in the North Atlantic. For such circulation (SGI > 0.2), higher temperatures found north of Iceland and colder conditions are found in the Labrador Sea (Fig. 4). Consistent with higher temperatures (SGI > 0.2) north of Iceland, the sea ice cover is reduced by 5%. The correlation of SGI with sea ice cover is −0.5 north of Iceland.

The time series of SGI over the last five centuries based on shell growth rates of the marine bivalve mollusk "All Iceland" (Fig. 2) are analyzed. In our analysis we concentrate on the power technique since it gave more consistent results linked to higher EPS values for the last 150 years (Fig. 1a). We note that the spline technique provides for more variability in the decadal band without changing the general structure (not shown). Our wavelet analysis indicates prominent oscillations around 12 to 20, around 20, and between 30 and 100 years, and weaker oscillations of 4 to 8 years (Fig. 5a,b,c). During

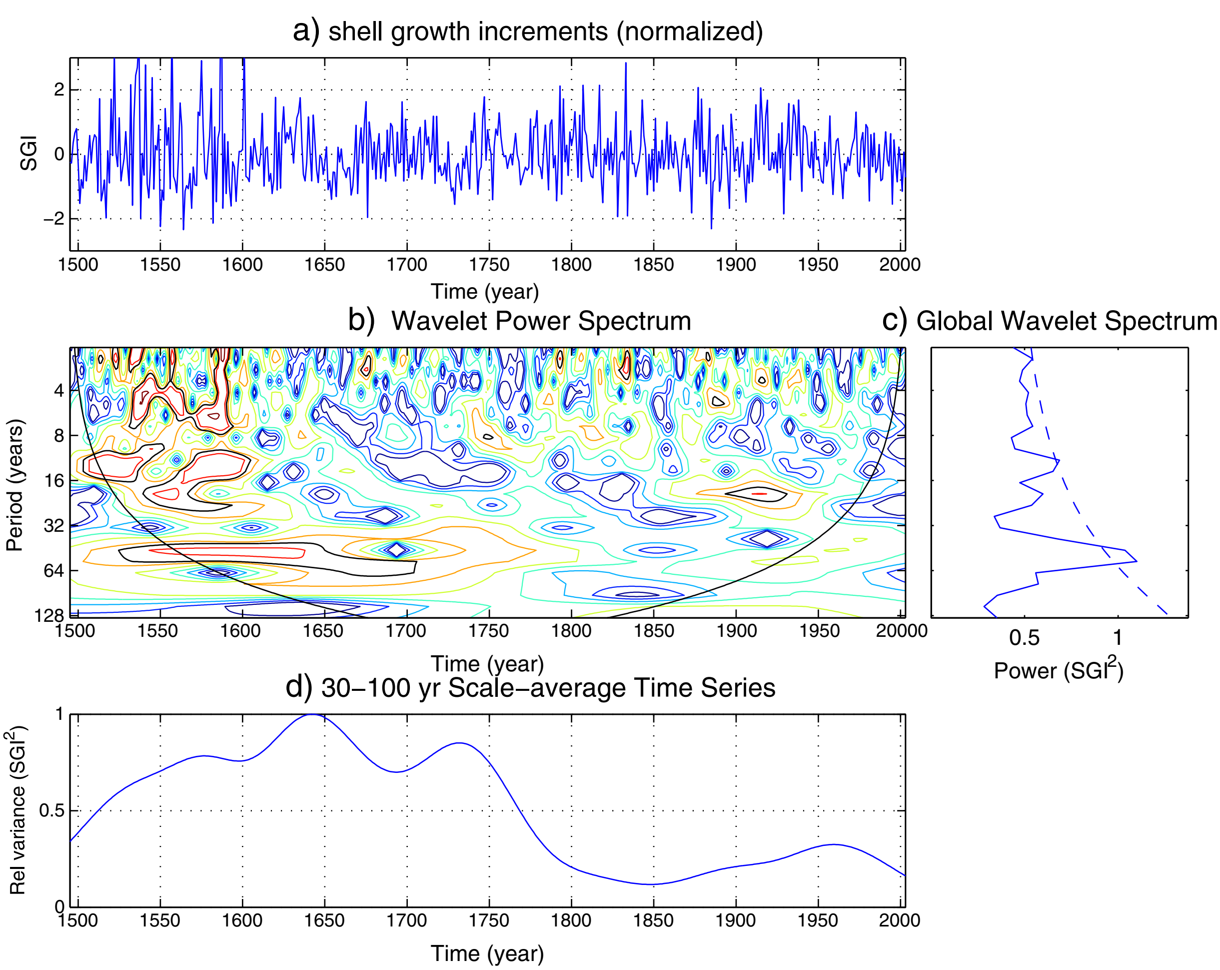

Fig. 5. a) Time series of SGI based on the power reconstruction of Fig. 2a. b) Morlet-6 wavelet spectrum with significant areas in interannual (1530–1600), quasi-decadal (mostly pronounced for 1500–1610), and interdecadal (1510–1770; 1860–1970) bands. Amplitudes are scaled with variance of the index. The logarithmic vertical axis indicates equivalent periods. The 90% confidence limits (based on the global wavelet in c) are given in thick contour lines. c) The power spectrum shows significant quasi-decadal and interdecadal peaks. The red noise background spectrum is calculated from an AR(1) process and lag-1 autocorrelation of SGI. d) The panel indicates strong level of variations on interdecadal time scales for the period 1520 to 1770.

the 16th century, quasi-decadal (12 to 16 years) variability in shell growth was on the order of twice that measured over the following four centuries (Fig. 5b). The strongest multidecadal variability is observed between 1550 and 1750 (Fig. 5d).

For decadal and multidecadal time scales, we calculated the 10-year (Fig. 6a) and 30-year (Fig. 6b) low-pass filtered values and calculated the correlation with SLP fields. The associated SLP map emphasizes a pattern with low pressure center above Greenland and a high pressure over Western Europe and the eastern North Atlantic Ocean (Fig. 6). Consistent with this, we find high values over Europe based on the Luterbacher et al. (2002) data in the multidecadal component (not shown). In order to determine the SLP variability modes on decadal time scales, we calculate the dominant empirical orthogonal functions (EOFs). The first mode (29% of the variance) represents an NAO-like pattern, whereas the second mode is a more blocking-like mode similar to the pattern shown in Fig. 6 explaining 16% of the variance. Performing an EOF analysis for long-term 30-year low-pass filtered SLP data (Luterbacher et al., 2002), the second modes become the dominating EOF (40% of the variance). A similar SLP structure was associated with the Atlantic Multidecadal Oscillation (Dima and Lohmann, 2007).

The multidecadal SST correlation field indicates a characteristic quasi-monopolar structure in the North Atlantic and regions of opposite sign in the Southern Hemisphere (Fig. 7). Significant areas are mainly in the northern North Atlantic Ocean. As indicated by several numerical experiments (e.g., Knight et al., 2005; Latif et al., 2004; Lohmann, 2003), such an SST structure can be associated with large-scale ocean circulation variations.

Long-term instrumental records are rare to establish our finding that the multidecadal variability is higher for the first part of the SGI record. Therefore, we display the variability of a long-term SST record based on alkenones (Sicre et al., 2002) covering the latest Holocene. Fig. 8 indicates enhanced SST variability in the multidecadal (30–100 years) band for 1500–1780 consistent with our record.

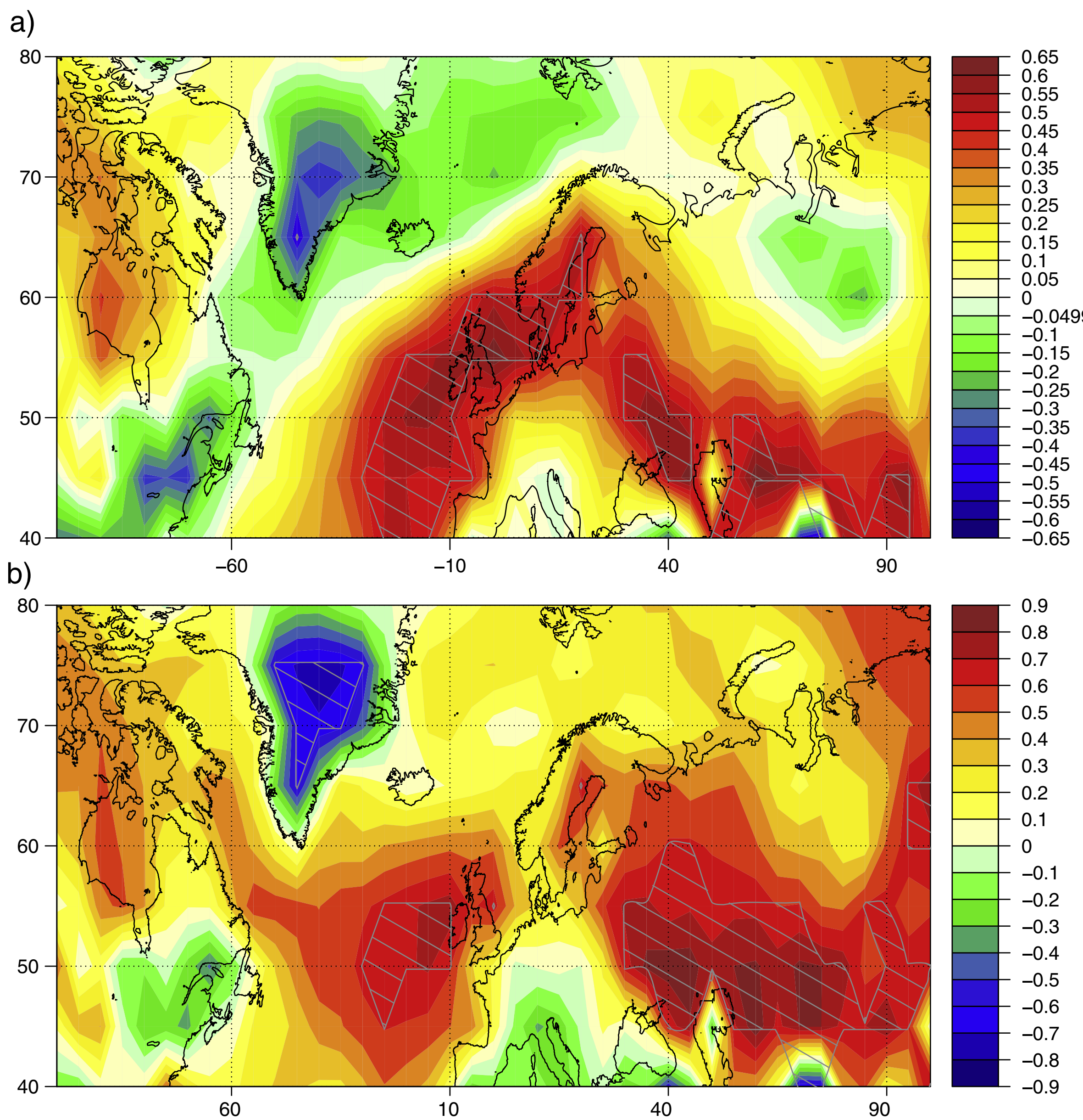

Fig. 6. Correlation of (a) 10-year and (b) 30-year low-pass filtered SGI with SLP when taking the SLP data set of Trenberth and Paolino (1980). Significant areas are striped.

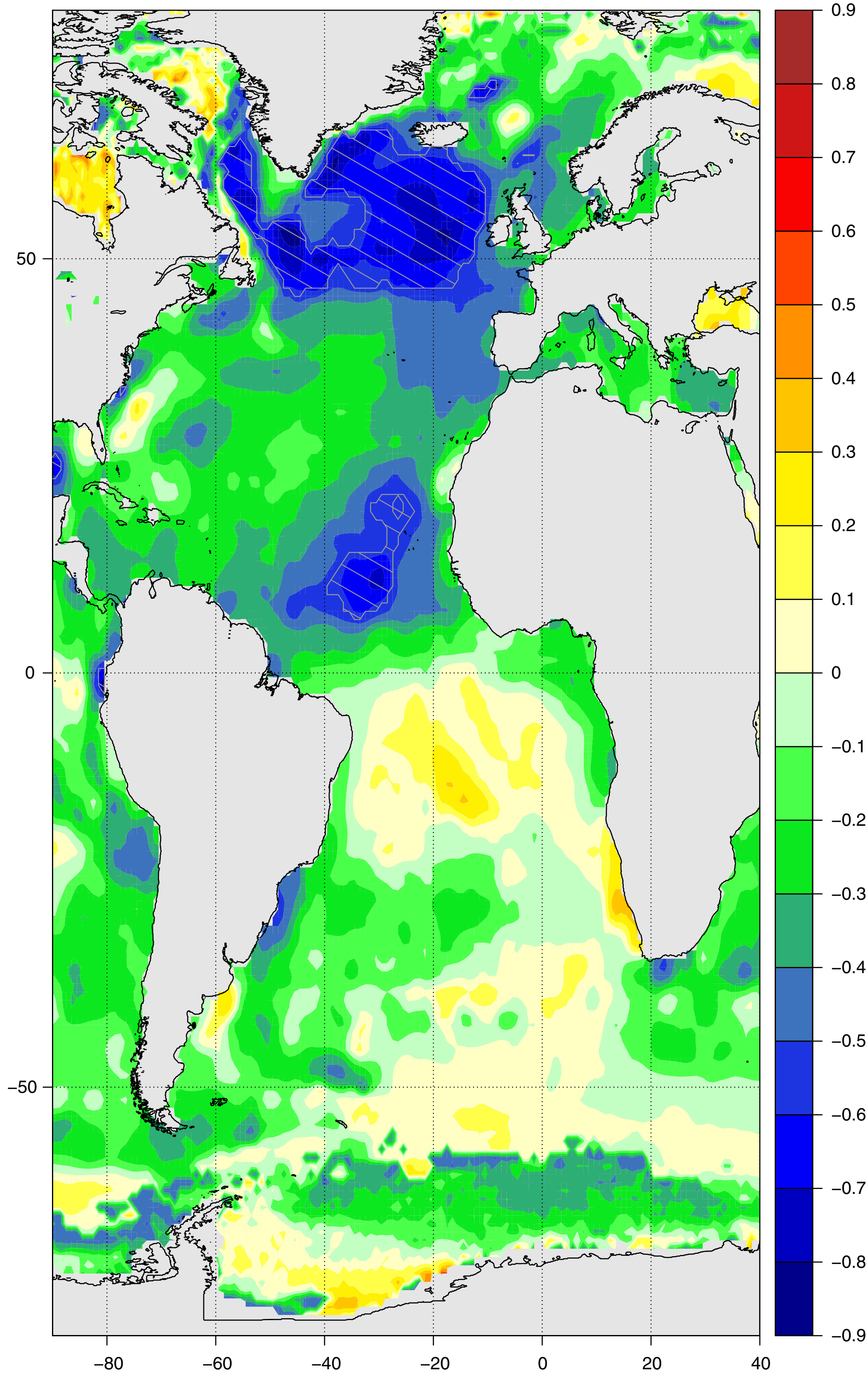

Fig. 7. Correlation SST map for SGI values (related to the power reconstruction of Fig. 2a) in the 30-year low-pass filtered band based on HadSST2 (Rayner et al., 2006). Significant areas are striped.

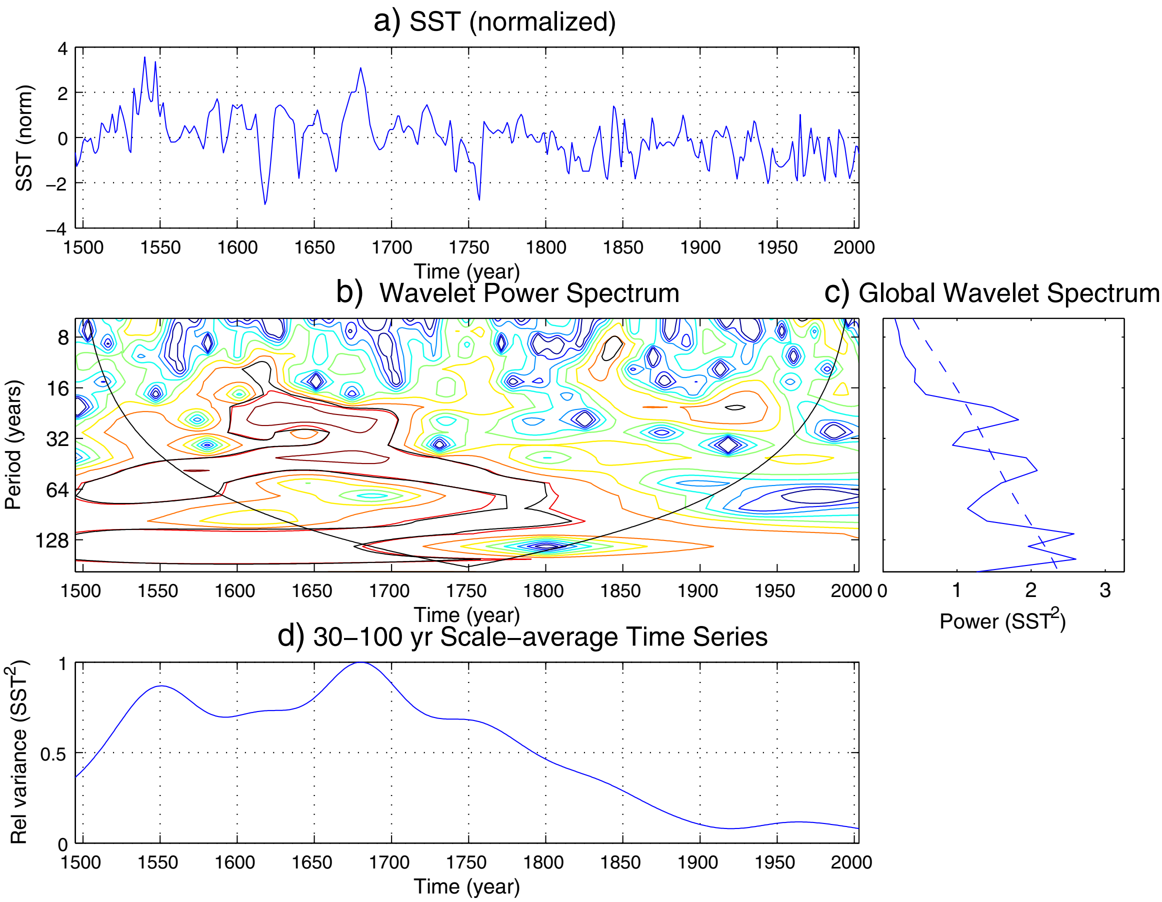

Fig. 8. a) Alkenone time series of Sicre et al. (2002). b) Morlet-6 wavelet spectrum with significant areas in quasi-decadal (mostly pronounced for 1600–1700, and 1900–1950), and interdecadal (1500–1800) bands. Amplitudes are scaled with variance of the index. The logarithmic vertical axis indicates equivalent periods. The 90% confidence limits (based on the global wavelet in c are given in thick contour lines. c) The power spectrum shows significant quasi-decadal and interdecadal peaks. The red noise background spectrum is calculated from an AR(1) process and lag-1 autocorrelation of SGI. d) The panel indicates strong level of variations on interdecadal time scales for the period 1500 to 1800.

4. Discussion

The observed correlation between shell growth of *A. islandica* and climate parameters underscores previous findings on the link between climate variability and ecological dynamics. We concentrate here on the decadal and multi-decadal variability. Fluctuations in circulation patterns are concurrent with changes in sea level pressure, temperature and sea ice. In turn, these environmental variables likely exert a great influence on growth of bivalve mollusks (Gunter, 1957). Less sea ice, and a tendency for stronger blocking of the atmosphere (favoring higher food supply) re-occur at decadal time periods and increase shell growth of *A. islandica*. Other hypotheses are related to wind, ocean circulation and food dynamics on shell growth (Ambrose et al., 2012; Carroll et al., 2011) which is probably also modulated on these time scales.

We tested several climate pattern and found robust results when shifting the months (not shown). It is likely that this robustness on long time scales is due to the memory in the system during colder months because the winter and early spring signal can survive in the subsurface layers.

As seen in the wavelet spectrum (Fig. 5b), cycle strength and frequency of shell growth vary through time. We observed a progressive shift from quasi- (12 to 16 years) to multi-decadal (20, 30 and 50 years) modes from the 16th to the late 18th century and from the early 19th century to modern times. At ~1820, the time interval dominated by the low frequency mode was abruptly followed by the 12- to 16-year mode. Quasi-decadal oscillations prevail during the 16th and 19th centuries, whereas multidecadal cycles occur predominantly 1600–1800 AD and during the 20th century. Quasi-decadal variability is followed by multidecadal variability (~1600 and ~1860). The methods provide an inherent uncertainty related to long time scales. However, as seen in independent SST data from the same area (Fig. 8), the change in variance over time seems to be a robust feature when looking for the last 500 years.

Pronounced variability in the 12 to 16 and 20-year bands has been documented in detail for the instrumental period (Deser and Blackmon, 1993; Dima and Lohmann, 2004). Deser and Blackmon (1993) demonstrated that the wintertime SSTs, the sea-ice and the atmospheric fluctuations over the subpolar gyre, change synchronously on the decadal time scale (10–15 years). The sign of anomalies indicates that quasi-decadal changes in SST and SLP over the subpolar and subtropical Atlantic gyres mark coupled ocean–atmosphere interactions (Kushnir, 1994; Park and Latif, 2005). According to the 509-year shell record, quasi-decadal climate variability was most pronounced during the 16th century. This observation is corroborated by historical documents (Ogilvie and Jónsson, 2001) and other climate proxies which indicate an extraordinarily variable climate and a significant increase in wind stress (Christiansen, 1998) in northern latitudes near the beginning of the Little Ice Age (Lamb, 1965; Trouet et al., 2012).

It is likely that the mean climate during the 16th century has resulted in a more vigorous quasi-decadal ocean, atmospheric circulation and sea ice export, which may explain the prevalence of 12 to 16 and 20-year modes in the shell record. Alternatively, this quasi-decadal mode might be associated to a new mode of operation related to the background climate. Yoshimori et al. (2010) present a persistent, decadal oscillation in a coupled atmosphere–ocean general circulation model under cold conditions, which is linked to anomalous subpolar gyre circulation and sea ice. While the exact mechanisms of this mode may be model dependent, it shows the possibility of a stronger oscillatory mode under different background conditions. It is conceivable that the documented highly variable climate as shown here is related to a transition from the warm to the cold climate of the Little Ice Age, in a similar way to that described by Hyde and Crowley (2002) in a context of multi-millennial climate variability.

One drawback of our “All Iceland” chronology is that we have just 2–3 chronologies and we have to be careful with the discussion of variance. Variance stabilization methods (Osborn et al., 1997) could be applied to adjust for bias in variance caused by changes in sample depth through time. However, this method is only applicable to time intervals where a sufficient number of SGI series is available, i.e. in the 20th century. Therefore, it has to remain unanswered if the observed larger year-to-year variance in time of major regime shifts (e.g., 16th century) is true or result of low sample number. Butler et al. (2012, this issue) also noted an increased year-to-year variance between the Medieval Climate Anomaly and the Little Ice Age. Here, we show independent evidence of increased multi-decadal variability in the early part of the “All Iceland” chronology and the analysis of SST reconstructions (Sicre et al., 2002). Consistent with the increased variability with cold climate, Wei and Lohmann (2012) found in a modeling study that the amplitude of the multidecadal oscillation increases when the mean overturning strength is reduced and when the system is more vulnerable. It is likely that the wind stress and storminess is largely affected in colder states (Lohmann, 2003; Trouet et al., 2012) possibly affecting SGI.

The dynamics of the variability mode in SGI can be related to regional temperature and sea ice characteristics, and are possibly related to an atmosphere–ocean feedback in the North Atlantic (Wanner et al., 2001, and references therein). Interestingly, it has been documented that anomalous SSTs near the coast of Newfoundland (as seen in Fig. 7) can significantly affect the atmospheric circulation in winter and spring (Barnston and Livezey, 1987; Palmer and Sun, 1985; Ratcliffe and Murray, 1970). Indeed, a positive SLP anomaly over the North Atlantic for winter and spring is consistent with earlier findings (Peng and Mysak, 1993; Peng et al., 1995). This circulation in turn provides for a northward displacement of the Gulf Stream (Frankignoul et al., 2001). An EOF analysis shows that the signature of SGI is related to the second EOF in SLP. Skeje (2000) found that the second EOF has a high temporal correlation with the sensible heat loss of the Nordic Seas. This in turn correlates well with the sea ice and Eurasian surface air temperature anomalies.

SGI variability on multidecadal time scales is strongly pronounced during 1600–1800, a period of equatorward expansion of sea ice (Ogilvie and Jónsson, 2001) which is most likely linked to enhanced southward sea ice export and more vigorous variability (Fig. 5). This is also consistent with Massé et al. (2008) indicating increased sea ice off north Iceland after 1600 is clearly shown by paleoceanographic data. A retreat of sea ice, associated with mild climates north of Iceland is consistent with the lower frequency mode of SGI (Fig. 5). The low-frequency variations of the Iceland sea ice extent anomaly are also consistent with a recent reconstruction of the Fram Strait sea ice export (Schmith and Hansen, 2003). Due to its prominence and spreading path along east Greenland, the Great Salinity Anomaly in the late 1960s represented a significant forcing reaching the Labrador Sea convection region (Dickson et al., 1988). It was the first event in a series of several significant salinity anomalies with decreasing amplitudes ending in the late 1990s. Anomalous strong sea-ice export from the Arctic through Fram Strait, associated with the Great Salinity Anomalies (Schmith and Hansen, 2003), would increase the freshwater fluxes in the North Atlantic (Hilmer et al., 1998) and can modulate the North Atlantic deep water formation (Häkkinen, 1999; Mauritzen and Häkkinen, 1997).

Besides internal variability as discussed here, there might be external influences on SGI. Schöne et al. (2005a) mention extremely low shell growth rates during 1816–1818 which are possibly the result of the environmental disturbances and reduced food supply caused by a volcanic eruption of Mount Tambora in 1815 (Robock, 2001). A similar relation is found for several major tropical eruptions between 1580 and 1600, falling within a period of extraordinarily harsh and highly variable climate in Iceland (Ogilvie and Jónsson, 2001). More frequent shifts between temperature extremes during this period may have also influenced primary productivity. The exact synoptic view for these events will be subject of a future study.

5. Conclusions

We show that variations in annual shell growth around northeastern Iceland are significantly related to several climate variables. In order to understand the physical mechanisms behind SGI variability, we evaluate composite maps of sea level pressure fields. Negative SLP anomalies dominate around Greenland while positive SLP anomalies prevail over Europe during high values of increments (a blocking situation). A reverse pattern occurs during years with low increments in the shell. Along with high SGI, we find less sea ice and increased temperatures north of Iceland. We suppose that under such conditions, food levels are higher, supporting faster shell growth. The composite map of SLP emphasizes a regional circulation pattern over the North Atlantic realm. For relative high values of SGI, enhanced blocking over Europe and advection from southwest is detected (arrows). We evaluated the statistical link between SGI and climate and therefore cannot explore the exact mechanism because of the lack of a sufficiently detailed coupled model linking climate with biology/ecology.

Compared to the NAO pattern, the SLP main pressure centers are tilted with an axis of the dipolar pattern inclined northeast to southwest. This structure represents a breakdown in the westerly zonal flow through a region. Such blocking-like structures impede the zonal flow in a limited sector of the atmosphere. Often, however, such blocks will eventually spread across large areas of the hemisphere. Atmospheric blocking is a large-scale mid-latitude atmospheric phenomenon that induces significant climate anomalies over various regions of the North Atlantic realm. Several studies (Barriopedro et al., 2006; Luo and Wan, 2005; Rimbu and Lohmann, 2011; Shabbar et al., 2001) detected pronounced decadal variability in atmospheric blocking frequency with imprints of the upper ocean structure in winter and spring (e.g., Barnston and Livezey, 1987; Palmer and Sun, 1985; Ratcliffe and Murray, 1970).

Observed surface temperature data over the last century shows strong variability at multidecadal time scales. In our record, we find enhanced variability of the proxy at the same time scales, and it appears that this oscillation had high amplitudes when the climate was relatively cold. The link between SGI and climate might be related to sea ice. Changes in food supply may result from variations in primary productivity (Dickson, 1999). Interestingly, the SLP signature is in phase with a wave structure that favors ice export variance in dynamic–thermodynamic sea ice models (Cavalieri, 2002). This connection on longer time scales is examined in instrumental data (Dima and Lohmann, 2007) indicating that the climate shift in the 1970s can be part of a quasi-periodic behavior on multidecadal time scales. Grosfeld et al. (2007) found an analog SLP response to Atlantic multidecadal SST forcing in a twenty ensemble member integration, indicating a deterministic response to SST anomalies. One can speculate that this circulation change supports increased sea ice export from the Arctic to the North Atlantic in a similar way to that suggested by Hilmer and Jung (2000). The sea ice export can influence the freshwater budget in the northern North Atlantic affecting salinity and ocean circulation (Dickson et al., 1988). It is conceivable that these climate oscillations linked to sea-ice export were a more pronounced feature during times when the climate was relatively cold. The reduced influence of warm and moist air from the sea during periods when the winters were relatively severe in Europe indicates that blocking was a prominent feature of North Atlantic climate. *A. islandica* records this phenomenon over centuries. As a logical next step, we will analyze more high-resolution proxy data covering the last millennium to identify decadal to multidecadal variability as recorded here.

Acknowledgments

Specimens of *A. islandica* were kindly provided by Wolfgang Dreyer, Zoological Museum of the University of Kiel, and Alda Möller (Ministry of Fisheries and Agriculture, Reykjavìk, Iceland). We thank Marie-F. Sicre for providing us the reconstructed SST data. Funding is through the PACES Program of the Helmholtz Society (GL). BRS gratefully acknowledges a research grant (SCHO793/4) by the German Research Foundation (DFG). The authors acknowledge very constructive suggestions from the two referees.

References

Ambrose, W., Renaud, P., Locke, W., Cottier, F., Berge, J., Carroll, M., Levin, B., Ryan, S., 2012. Growth line deposition and variability in growth of two circumpolar bivalves (*Serripes groenlandicus* and *Clinocardium ciliatum*). Polar Biology 35, 345–354.
Appenzeller, C., Stocker, T.F., Anklin, M., 1998. North Atlantic Oscillation dynamics recorded in Greenland ice cores. Science 282, 446–449.
Barnston, A.G., Livezey, R.E., 1987. Classification, seasonality and persistence of low-frequency atmospheric circulation patterns. Monthly Weather Review 115, 1083–1126.
Barriopedro, D., Herrera, R.G., Lupo, A.R., Hernandez, E., 2006. A climatology of Northern Hemisphere blocking. Journal of Climate 19, 1042–1063.
Bjerknes, J., 1964. Atlantic air–sea interaction. Advances in Geophysics 10, 1–82.
Briffa, K., Jones, P., 1990. Basic chronology statistics and assessment. In: Cook, E., Kairiukstis, L. (Eds.), Methods of Dendrochronology: Applications in the Environmental Sciences. Kluwer Academic, Dordrecht, pp. 137–152.
Butler, P.G., Richardson, C., Scourse, J.D., Wanamaker Jr., A.D., Shammon, T.M., Bennell, J.D., 2010. Marine climate in the Irish Sea: analysis of a 489 year marine master chronology derived from growth increments in the shell of the clam *Arctica islandica*. Quaternary Science Reviews 29, 1614–1632.
Butler, P.G., Wanamaker Jr., A.D., Scourse, J.D., Richardson, C.A., Reynolds, D.J., 2012. Variability of marine climate on the North Icelandic Shelf in a 1357-year proxy archive based on growth increments in the bivalve *Arctica islandica*. Palaeogeography, Palaeoclimatology, Palaeoecology. http://dx.doi.org/10.1016/j.palaeo.2012.01.016.
Carroll, M.L., Ambrose Jr., W.G., Levin, B.S., Ryan, S.K., Ratner, A.R., Henkes, G.A., Greenacre, M.J., 2011. Climatic regulation of *Clinocardium ciliatum* (Bivalvia) growth in the northwestern Barents Sea. Palaeogeography, Palaeoclimatology, Palaeoecology. http://dx.doi.org/10.1016/j.palaeo.2010.06.001.
Cavalieri, D.J., 2002. A link between Fram Strait sea ice export and atmospheric planetary wave phase. Geophysical Research Letters 29, 1614. http://dx.doi.org/10.1029/2002GL014684.
Christiansen, H.H., 1998. 'Little Ice Age' nivation activity in northeast Greenland. The Holocene 8, 719–728.
Compo, G.P., Whitaker, J.S., Sardeshmukh, P.D., Matsui, N., Allan, R.J., Yin, X., Gleason, B.E., Vose, R.S., Rutledge, G., Bessemoulin, P., Brönnimann, S., Brunet, M., Crouthamel, R.I., Grant, A.N., Groisman, P.Y., Jones, P.D., Kruk, M., Kruger, A.C., Marshall, G.J., Maugeri, M., Mok, H.Y., Nordli, Ø., Ross, T.F., Trigo, R.M., Wang, X.L., Woodruff, S.D., Worley, S.J., 2011. The twentieth century reanalysis project. Quarterly Journal of the Royal Meteorological Society 137, 1–28. http://dx.doi.org/10.1002/qj.776.
Methods of dendrochronology. In: Cook, E.R., Kairiukstis, L.A. (Eds.), Applications in the Environmental Sciences. Kluwer, Dordrecht, Netherlands (394 pp.).
Dahlgren, T.G., Weinberg, J.R., Halanych, K.M., 2000. Phylogeography of the ocean quahog (*Arctica islandica*): influences of paleoclimate on genetic diversity and species range. Marine Biology 137, 487–495.
Delworth, T.L., Mann, M.E., 2000. Observed and simulated multidecadal variability in the Northern Hemisphere. Climate Dynamics 16, 661–676.
Deser, C., Blackmon, M., 1993. Surface climate variations over the North Atlantic Ocean during winter: 1900–1989. Journal of Climate 6, 1743–1753.
Dickson, R.R., 1999. All change in the Arctic. Nature 397, 389–391.
Dickson, R.R., Meincke, J., Malmberg, S.-A., Lee, A.J., 1988. The 'Great Salinity Anomaly' in the northern North Atlantic 1968–1982. Progress in Oceanography 20, 103–151.
Dima, M., Lohmann, G., 2004. Fundamental and derived modes of climate variability. Application to biennial and interannual timescale. Tellus 56, 229–249.
Dima, M., Lohmann, G., 2007. A mechanism for the Atlantic Multidecadal Oscillation. Journal of Climate 20, 2706–2719.
Eden, C., Jung, T., 2001. North Atlantic interdecadal variability: oceanic response to the North Atlantic Oscillation (1865–1997). Journal of Climate 14, 676–691.
Enfield, D., Mayer, D., 1997. Tropical Atlantic sea surface temperature variability and its relation to El Niño-Southern Oscillation. Journal of Geophysical Research 102 (C1). http://dx.doi.org/10.1029/96JC03296.
Esper, J., Cook, E.R., Krusic, P.J., Peters, K., Schweingruber, F.H., 2003. Tests of the RCS method for preserving low-frequency variability in long tree-ring chronologies. Tree-Ring Research 59, 81–98.
Frankignoul, C., Hasselmann, K., 1977. Stochastic climate models. Part II: application to sea-surface temperature anomalies and thermocline variability. Tellus 29, 284–305.
Frankignoul, C., Coëtlogon de, G., Joyce, T.M., Dong, S., 2001. Gulf Stream variability and ocean–atmosphere interactions. Journal of Physical Oceanography 31, 3516–3529.
Fritts, H.C., 1976. Tree Rings and Climate. Academic Press, London . (xii + 567 pp.).
Grissino-Mayer, H.D., 2001. Evaluating crossdating accuracy: a manual and tutorial for the computer program COFECHA. Tree-ring research 57, 205–221.
Grosfeld, K., Lohmann, G., Rimbu, N., Fraedrich, K., Lunkeit, F., 2007. Atmospheric multidecadal variations in the North Atlantic realm: proxy data, observations, and atmospheric circulation model studies. Climate of the Past 3, 39–50.
Gunter, G., 1957. Temperature. Memoir — Geological Society of America 67, 159–184.
Häkkinen, S., 1999. A simulation of thermohaline effects of a Great Salinity Anomaly. Journal of Climate 12, 1781–1795.
Häkkinen, S., Rhines, P.B., Worthen, D.L., 2011. Atmospheric blocking and Atlantic multi-decadal ocean variability. Science 334, 655–659.
Hasselmann, K., 1974. On the spectral dissipation of ocean waves due to whitecapping. Boundary-Layer Meteorology 126, 107–127.
Hasselmann, K., 1976. Stochastic climate models. Part I. Theory. Tellus 28, 473–484.
Hetzinger, S., Pfeiffer, M., Dullo, W.C., Keenlyside, N., Latif, M., Zinke, J., 2008. Caribbean coral tracks Atlantic Multidecadal Oscillation and past hurricane activity. Geology 36, 11–14.
Hilmer, M., Jung, T., 2000. Evidence for a recent change in the link between the North Atlantic Oscillation and Arctic sea ice export. Geophysical Research Letters 27, 989–992.
Hilmer, M., Harder, M., Lemke, P., 1998. Sea ice transport: a highly variable link between Arctic and North Atlantic. Geophysical Research Letters 25, 3359–3362.
Hurrell, J.W., 1995. Decadal trends in the North Atlantic Oscillation: regional temperatures and precipitation. Science 269, 676–679.
Hurrell, J.W., van Loon, H., 1997. Decadal variations associated with the North Atlantic Oscillation. Climatic Change 36, 301–326.
Hyde, W.T., Crowley, T.J., 2002. Stochastic forcing of Pleistocene ice sheets: implications for the origin of millennial-scale climate oscillations. Paleoceanography 17, 1067. http://dx.doi.org/10.1029/2001PA000669.
Jansen, E., Overpeck, J., Briffa, K.R., Duplessy, J.-C., Joos, F., Masson-Delmotte, V., Olago, D., Otto-Bliesner, B., Peltier, W.R., Rahmstorf, S., Ramesh, R., Raynaud, D., Rind, D., Solomina, O., Villalba, R., Zhang, D., 2007. Palaeoclimate. In: Solomon, S., Qin, D., Manning, M., Chen, Z., Marquis, M., Averyt, K.B., Tignor, M., Miller, H.L. (Eds.), Climate Change 2007: The Physical Science Basis. : Contribution of Working Group I to the Fourth Assessment Report of the Intergovernmental Panel on Climate Change. Cambridge University Press, Cambridge, United Kingdom and New York, NY, USA, pp. 433–497.
Jones, D.S., 1980. Annual cycle of shell growth increment formation in two continental shelf bivalves and its paleoecologic significance. Paleobiology 6, 331–340.
Jones, D.S., Arthur, M.A., Allard, D.J., 1989. Sclerochronological records of temperature and growth from shells of *Mercenaria mercenaria* from Narragansett Bay, Rhode Island. Marine Biology 102, 225–234.
Kalnay, E., Kanamitsu, M., Kistler, R., Collins, W., Deaven, D., Gandin, L., Iredell, M., Saha, S., White, G., Woollen, J., Zhu, Y., Leetmaa, A., Reynolds, R., Chelliah, M., Ebisuzaki, W., Higgins, W., Janowiak, J., Mo, K.C., Ropelewski, C., Wang, J., Jenne, R., Joseph, D., 1996. The NCEP/NCAR 40-year reanalysis project. Bulletin of the American Meteorological Society 77, 437–471.
Kim, J.-H., Rimbu, N., Lorenz, S.J., Lohmann, G., Nam, S.-I., Schouten, S., Rühlemann, C., Schneider, R.R., 2004. North Pacific and North Atlantic sea-surface temperature variability during the Holocene. Quaternary Science Reviews 23, 2141–2154.
Knight, J.R., Allan, R.J., Folland, C.K., Vellinga, M., Mann, M.E., 2005. A signature of persistent natural thermohaline circulation cycles in observed climate. Geophysical Research Letters 32, L20708. http://dx.doi.org/10.1029/2005GL024233.
Knudsen, M.F., Seidenkrantz, M.-S., Jacobsen, B.H., Kuijpers, A., 2011. Tracking the Atlantic Multidecadal Oscillation through the last 8,000 years. Nature Communications 2, 178. http://dx.doi.org/10.1038/ncomms1186.
Kushnir, Y., 1994. Interdecadal variations in North Atlantic sea surface temperature and associated atmospheric conditions. Journal of Climate 7, 141–157.
Lamb, H.H., 1965. The early medieval warm epoch and its sequel. Palaeogeography, Palaeoclimatology, Palaeoecology 1, 13–37.
Latif, M., Roeckner, E., Botzet, M., Esch, M., Haak, H., Hagemann, S., Jungclaus, J., Legutke, S., Marsland, S., Mikolajewicz, U., Mitchell, J., 2004. Reconstructing, monitoring, and predicting multidecadal-scale changes in the North Atlantic thermohaline circulation with sea surface temperature. Journal of Climate 17, 1605–1614.
Lohmann, G., 2003. Atmospheric and oceanic freshwater transport during weak Atlantic overturning circulation. Tellus 55, 438–449.
Lohmann, G., Rimbu, N., Dima, M., 2004. Climate signature of solar irradiance variations: analysis of long-term instrumental and historical data. International Journal of Climatology 24, 1045–1056.
Luo, D., Wan, H., 2005. Decadal variability of wintertime North Atlantic and Pacific blockings: a possible cause. Geophysical Research Letters 32, L23810. http://dx.doi.org/10.1029/2005GL024329.
Luterbacher, J., Xoplaki, E., Dietrich, D., Rickli, R., Jacobeit, J., Beck, C., Gyalistras, D., Schmutz, C., Wanner, H., 2002. Reconstruction of sea level pressure fields over the eastern North Atlantic and Europe back to 1500. Climate Dynamics 18, 545–561.
Mann, M., 2004. On smoothing potentially non-stationary climate time series. Geophysical Research Letters 31, L07214. http://dx.doi.org/10.1029/2004GL019569.
Mann, M.E., Park, J., Bradley, R.S., 1995. Global interdecadal and century-scale climate oscillations during the past five centuries. Nature 378, 266–270.

Maraun, D., Kurths, J., 2004. Cross wavelet analysis: significance testing and pitfalls. Nonlinear Processes in Geophysics 11, 505–514.

Marchitto, T.A., Jones, G.A., Goodfriend, G.A., Weidman, C.R., 2000. Precise temporal correlation of Holocene mollusk shells using sclerochronology. Quaternary Research 53, 236–246.

Massé, G., Rowland, S.J., Sicre, M.-A., Jacob, J., Jansen, E., Belt, S.T., 2008. Abrupt climate changes for Iceland during the last millennium: evidence from high resolution sea ice reconstructions. Earth and Planetary Science Letters 269, 565–569.

Mauritzen, C., Häkkinen, S., 1997. Sensitivity of thermohaline circulation to sea-ice forcing in an Arctic–North Atlantic model. Journal of Geophysical Research 24, 3257–3260.

Nicol, D., 1951. Recent species of the veneroid pelecypod *Arctica*. Journal of the Washington Academy of Sciences 41, 102–106.

Ogilvie, A.E.J., Jónsson, T., 2001. Little Ice Age research: a perspective from Iceland. Climatic Change 48, 9–52.

Osborn, T.J., Briffa, K.R., Jones, P.D., 1997. Adjusting variance for sample-size in tree-ring 787 chronologies and other regional-mean time-series. Dendrochronologia 15, 89–99.

Palmer, T.N., Sun, Z., 1985. A modelling and observational study of the relationship between sea surface temperature in the northwest Atlantic and atmospheric general circulation. Quarterly Journal of the Royal Meteorological Society 111, 947–975.

Park, W., Latif, M., 2005. Ocean dynamics and the nature of air–sea interactions over the North Atlantic. Journal of Climate 18, 982–995.

Peng, S., Mysak, L.A., 1993. A teleconnection study of interannual sea surface temperature fluctuation in the northern North Atlantic and precipitation and runoff over western Siberia. Journal of Climate 6, 876–885.

Peng, S., Mysak, L.A., Ritchie, H., Derome, J., Dugas, B., 1995. The difference between early and midwinter atmospheric response to sea surface temperature anomalies in the northwest Atlantic. Journal of Climate 8, 137–157.

Poore, H.R., White, N., Jones, S., 2009. A Neogene chronology of Iceland plume activity from V-shaped ridges. Earth and Planetary Science Letters 283, 113.

Ratcliffe, R.A.S., Murray, R., 1970. New lag associations between North Atlantic sea temperatures and European pressure applied to long-range forecasting. Quarterly Journal of the Royal Meteorological Society 96, 226–246.

Rayner, N.A., Brohan, P., Parker, D.E., Folland, C.K., Kennedy, J.J., Vanicek, M., Ansell, T.J., Tett, S.F.B., 2006. Improved analyses of changes and uncertainties in sea surface temperature measured in situ since the mid-nineteenth century: the HadSST2 data set. Journal of Climate 19, 446–469.

Rimbu, N., Lohmann, G., 2011. Winter and summer blocking variability in the North Atlantic region evidence from long-term observational and proxy data from southwestern Greenland. Climate of the Past 7, 543–555.

Robock, A., 2001. Volcanic eruption, Tambora. In: Munn, T. (Ed.), Encyclopedia of Global Environmental Change, vol. 1. John Wiley and Sons, London, pp. 737–738.

Ropes, J.W., Murawski, S.A., 1983. Maximum shell length and longevity in ocean Quahogs, *A. islandica* Linné. ICES/C.M., K:32. Shellfish Communication (8 pp.).

Schlesinger, M.E., Ramankutty, N., 1994. An oscillation in the global climate system of period 65–70 years. Nature 367, 723–726.

Schmith, T., Hansen, C., 2003. Fram Strait ice export during the nineteenth and twentieth centuries reconstructed from a multiyear sea ice index from Southwestern Greenland. Journal of Climate 16, 2782–2792.

Schöne, B.R., 2008. The curse of physiology. Challenges and opportunities in the interpretation of geochemical data from mollusk shells. Geo-Marine Letters 28, 269–285.

Schöne, B.R., Fiebig, J., Pfeiffer, M., Gleß, R., Hickson, J., Johnson, A.L.A., Dreyer, W., Oschmann, W., 2005a. Climate records from a bivalved Methuselah (*Arctica islandica*, Mollusca; Iceland). Palaeogeography, Palaeoclimatology, Palaeoecology 228, 130–148.

Schöne, B.R., Pfeiffer, M., Pohlmann, T., Siegismund, F., 2005b. A seasonally resolved bottom water temperature record for the period of AD 1866–2002 based on shells of *Arctica islandica* (Mollusca, North Sea). International Journal of Climatology 25, 947–962.

Schöne, B.R., Dunca, E., Fiebig, J., Pfeiffer, M., 2005c. Mutvei's solution: an ideal agent for resolving microgrowth structures of biogenic carbonates. Palaeogeography, Palaeoclimatology, Palaeoecology 228, 149–166.

Shabbar, A., Huang, J., Higuchi, K., 2001. The relationship between the wintertime North Atlantic Oscillation and blocking episodes in the North Atlantic. International Journal of Climatology 21, 355–369.

Sicre, M.-A., Bard, E., Ezat, U., Rostek, F., 2002. Alkenone distributions in the North Atlantic and Nordic Sea surface waters. Geochemistry, Geophysics, Geosystems 3 (2), 2001GC000159, 1–13.

Skeje, P., 2000. Meridional flow variability over the Nordic Seas in the Arctic Oscillation framework. Geophysical Research Letters 27, 2569–2572.

Sutton, R.T., Allen, R.M., 1997. Decadal predictability in North Atlantic sea surface temperature and climate. Nature 388, 563–567.

Timmermann, A.M., Latif, M., Voss, R., Grótzner, A., 1998. Northern hemispheric interdecadal variability: a coupled air–sea mode. Journal of Climate 11, 1906–1931.

Torrence, C., Compo, G.P., 1998. A practical guide to wavelet analysis. Bulletin of the American Meteorological Society 79, 61–78.

Trenberth, K.E., Paolino, D.A., 1980. The Northern Hemisphere sea level pressure data set: trends, errors and discontinuities. Monthly Weather Review 108, 855–872.

Trouet, V., Esper, J., Graham, N.E., Baker, A., Scourse, J.D., Frank, D.C., 2009. Persistent positive North Atlantic Oscillation mode dominated the Medieval Climate Anomaly. Science 324, 78–80.

Trouet, V., Scourse, J.D., Raible, C.C., 2012. North Atlantic storminess and Atlantic meridional overturning circulation during the last Millennium: reconciling contradictory proxy records of NAO variability. Global and Planetary Change 84–85, 48–55.

von Storch, H., Zwiers, F.W., 1999. Statistical Analysis in Climate Research. Cambridge University Press, Cambridge . (496 pp.).

Wanamaker Jr., A.D., Heinemeier, J., Scourse, J.D., Richardson, C.A., Butler, P.G., Eiriksson, J., Knudsen, K.L., 2008. Very long-lived mollusks confirm 17th century AD tephra-based radiocarbon reservoir ages for North Icelandic Shelf waters. Radiocarbon 50, 399–412.

Wanamaker Jr., A.D., Kreutz, K.J., Schöne, B.R., Maasch, K.A., Pershing, A., Borns, H.W., Introne, D.S., Feindel, S., 2009. A late Holocene paleo-productivity record in the Western Gulf of Maine, USA, inferred from growth histories of the long-lived ocean quahog (*Arctica islandica*). International Journal of Earth Sciences 98, 19–29.

Wanamaker Jr., A.D., Kreutz, K.J., Schöne, B.R., Introne, D.S., 2011. Gulf of Maine shells reveal changes in seawater temperature seasonality during the Medieval Climate Anomaly and the Little Ice Age. Palaeogeography, Palaeoclimatology, Palaeoecology 302, 43–51.

Wanamaker, A.D., Butler, P.G., Scourse, J.D., Heinemeier, J., Eiriksson, J., Knudsen, K.L., 2012. Surface changes in the North Atlantic meridional overturning circulation during the last millennium. Nature Communications 3, 899.

Wanner, H., Brönnimann, S., Casty, C., Gyalistras, D., Luterbacher, J., Schmutz, C., Stephenson, D.B., Xoplaki, E., 2001. North Atlantic Oscillation — concepts and studies. Surveys in Geophysics 22, 321–382.

Wei, W., Lohmann, G., 2012. Simulated Atlantic Multidecadal Oscillation during the Holocene. Journal of Climate. http://dx.doi.org/10.1175/JCLI-D-11-00667.1.

Wei, W., Lohmann, G., Dima, M., 2012. Distinct modes of internal variability in the global meridional overturning circulation associated to the Southern Hemisphere westerly winds. Journal of Physical Oceanography 42, 785–801.

Weidman, C.R., Jones, G.A., Lohmann, K.C., 1994. The long-lived mollusc *Arctica islandica*: a new paleoceanographic tool for the reconstruction of bottom temperatures for the continental shelves of the northern North Atlantic Ocean. Journal of Geophysical Research-Oceans 99 (C9), 18305–18314.

Wigley, T.M.L., Briffa, K.R., Jones, P.D., 1984. On the average value of correlated time series, with applications in dendroclimatology and hydrometeorology. Journal of Climate and Applied Meteorology 23, 201–213.

Witbaard, R., Franken, R., Visser, B., 1997. Growth of juvenile *Arctica islandica* under experimental conditions. Helgoländer Meeresuntersuchungen 51, 417–431.

Yoshimori, M., Raible, C.C., Stocker, T.F., Renold, M., 2010. Simulated decadal oscillations of the Atlantic meridional overturning circulation in a cold climate state. Climate Dynamics 34, 101–121.